Lecture Notes in Applied and Computational Mechanics

Volume 55

For other titles published in this series, go to
www.springer.com/series/4623

René de Borst • Ekkehard Ramm
Editors

Multiscale Methods in Computational Mechanics

Progress and Accomplishments

Springer

Editors
René de Borst
Department of Mechanical Engineering
Eindhoven University of Technology
Eindhoven
The Netherlands
R.d.Borst@tue.nl

Ekkehard Ramm
Institute of Structural Mechanics
University of Stuttgart
Stuttgart
Germany

ISSN 1613-7736 e-ISSN 1860-0816
ISBN 978-90-481-9808-5 e-ISBN 978-90-481-9809-2
DOI 10.1007/978-90-481-9809-2
Springer Dordrecht Heidelberg London New York

Library of Congress Control Number: 2010935928

Cover design: eStudio Calamar S.L.

Printed on acid-free paper

Springer is part of Springer Science+Business Media (www.springer.com)

Table of Contents

Part 4: Coupled Problems and Porous Media

Preface

For a long time limited computational resources restricted the scale of observation and modeling of physical systems mostly to one scale in time and space. This modus operandi was accepted although it was well known that the response at the level of practical interest is to a large extent determined by processes that occur at scales which are one to several orders of a magnitude smaller, namely the meso, micro or even nanoscales. The rapid increase in computer power and the development of efficient computational methods allow coming closer to the human dream of a continuous model through all spatial and temporal scales. However seeking solutions using numerical models simultaneously at the various length scales has proven to be beyond current computational capabilities. This perception is the starting point for the development of Multiscale Methods which is currently one of the hot research topics all over the world. Multiscale Methods either derive properties at the level of observation by repeated numerical homogenization of more fundamental physical properties several scales below (upscaling), or they devise concurrent schemes where those parts of the domain that are of interest are computed with a higher resolution than parts that are of less interest or where the solution is varying only slowly.

The present volume contains selected papers presented at the International Colloquium on Multiscale Methods in Computational Mechanics in Rolduc, the Netherlands, on 11–13 March 2009 (MMCM 2009). The contributions in the first part address multiscale methods in Computational Fluid Dynamics; in particular turbulence modeling applying the Variational Multiscale Method is described. The second part deals with materials having a distinct microstructure such as single- and poly-crystals, granular materials, aggregates embedded in a matrix, micro-laminates and nano-composites. Part three focuses on materials and structures and the interaction between their behavior on micro/meso- and macro-scales. Failure of composites and laminates, material modeling of shotcrete in tunnels, buckling of paperboard on different scales as well as material and structural optimization are investigated. The fourth part concentrates on coupled problems and porous media like concrete and charged hydrated materials.

The mentioned colloquium was organized by the German–Dutch Research Unit "Multiscale Methods in Computational Mechanics", in which a group of scientists in Germany at Universität Stuttgart and TU München and in the Netherlands at TU

Delft and TU Eindhoven have joined forces in order to address a variety of problem areas and computational solution strategies for multiscale methods in mechanics of structures, materials and flows. This joint project, which serves as a prototype for research cooperations within Europe, was financially supported by the German Research Foundation (Deutsche Forschungsgemeinschaft, DFG FOG 509), The Netherlands Technology Foundation (STW) and The Netherlands Organization for Scientific Research (NWO). This support is very much appreciated.

We also would like to thank the authors very much for their valuable contributions. Furthermore our thanks go to Springer for taking over the publication of this volume in its LNACM series.

January 2010
René de Borst, Technische Universiteit Eindhoven
Ekkehard Ramm, Universität Stuttgart

List of Authors

Acartürk, Ayhan Y.
Universität Stuttgart, Institut für Mechanik (Bauwesen), Stuttgart, Germany
acar@mechbau.uni-stuttgart.de

Akkerman, Ido
University of California, San Diego, Department of Structural Engineering, USA
IAkkerman@ucsd.edu

Allix, Olivier
L.M.T., ENS de Cachan, France
allix@lmt.ens-cachan.fr

Aslan, Ozgur
Mines ParisTech, Centre des Matériaux, Evry, France
ozgur.aslan@ensmp.fr

Badia, Santiago
Universitat Politècnica de Catalunya, International Center for Numerical Methods in Engineering (CIMNE), Barcelona, Spain
sbadia@cimne.upc.edu

Bazilevs, Yuri
University of California, San Diego, Department of Structural Engineering, USA
yuri@ucsd.edu

de Borst, René
Eindhoven University of Technology, Department of Mechanical Engineering, Eindhoven, The Netherlands
R.d.Borst@tue.nl

Bruss, Ingrid
Universität Stuttgart, Institut für Baustatik und Baudynamik, Stuttgart, Germany
bruss@ibb.uni-stuttgart.de

Calo, Victor M.
KAUST, Earth and Environmental Science and Engineering, Saudi Arabia
victor.calo@kaust.edu.sa

Cid Alfaro, Marcela V.
Corus, IJmuiden, The Netherlands

Codina, Ramon
Universitat Politècnica de Catalunya, Departament de Resistencia de Materials i Estructures a l'Enginyeria, Barcelona, Spain
ramon.codina@upc.edu

Daxner, Thomas
CAE Simulations & Solutions, Wien, Austria
daxner@ilsb.tuwien.ac.at

Dettmar, Joachim
Universität Stuttgart, Institut für Mechanik (Bauwesen), Stuttgart, Germany

Dormieux, Luc
École Nationale des Ponts et Chaussées, Laboratoire des Matériaux et Structures du Génie Civil (LMSGC), Champs-sur-Marne, France
dormieux@lmsgc.enpc.fr

Doweidar, Mohamed H.
Centro PolitĆcnico Superior de Zaragoza, Área de Mecánica de Fluidos, Zaragoza, Spain

Ehlers, Wolfgang
Universität Stuttgart, Institut für Mechanik (Bauwesen), Stuttgart, Germany
ehlers@mechbau.uni-stuttgart.de

Erhart, Andrea
DYNAmore, Stuttgart, Germany
andrea.erhart@dynamore.de

Fish, Jacob
Rensselaer Polytechnic Institute, Multiscale Science and Engineering Center, Troy, NY, USA
fishj@rpi.edu

Flatscher, Thomas
Technische Universität Wien, Institut für Leichtbau und Struktur-Biomechanik, Wien, Austria
flatscher@ilsb.tuwien.ac.at

Forest, Samuel
Mines ParisTech, Centre des Matériaux, Evry, France
samuel.forest@ensmp.fr

Fuster, Daniel
Centro Politécnico Superior de Zaragoza, Área de Mecánica de Fluidos, Zaragoza, Spain

Gamnitzer, Peter
Technische Universität München, Lehrstuhl für Numerische Mechanik, München, Germany
gamnitzer@lnm.mw.tum.de

Gawin, Dariusz
TU Lodz, Department of Building Physics and Building Materials, Lodz, Poland
gawindar@p.lodz.pl

Geurts, Bernard J.
University of Twente, Mathematical Sciences, Enschede; Eindhoven University of Technology, Department of Applied Physics, Eindhoven, The Netherlands
b.j.geurts@utwente.nl

Gosselet, Pierre
L.M.T., ENS de Cachan, France
gosselet@lmt.ens-cachan.fr

Gravemeier, Volker
Technische Universität München, Lehrstuhl für Numerische Mechanik, München, Germany
vgravem@lnm.mw.tum.de

Hackl, Klaus
Ruhr-Universität Bochum, Lehrstuhl für Allgemeine Mechanik, Bochum, Germany
klaus.hackl@rub.de

Hauke, Guillermo
Centro Politécnico Superior de Zaragoza, Área de Mecánica de Fluidos, Zaragoza, Spain
ghauke@unizar.es

Hellmich, Christian
Technische Universität Wien, Institut für Mechanik der Werkstoffe und Strukturen, Wien, Austria
christian.hellmich@tuwien.ac.at

Hettich, Thomas M.
Mahle GmbH, Stuttgart, Germany

Hilchenbach, Frédéric
Universität Stuttgart, Institut für Baustatik und Baudynamik, Stuttgart, Germany
hilchenbach@ibb.uni-stuttgart.de

Hughes, Thomas J.R.
The University of Texas at Austin, Institute for Computational Engineering and Sciences, Austin, USA
hughes@ices.utexas.edu

Hulshoff, Steven J.
Delft University of Technology, Aerospace Engineering, Delft, The Netherlands
s.j.hulshoff@tudelft.nl

Huyghe, Jacques M.R.
Eindhoven University of Technology, Department of Biomedical Engineering, Eindhoven, The Netherlands
j.m.r.huyghe@tue.nl

Jeannin, Laurent
Gaz de France (GDF), France

Kato, Junji
Universität Stuttgart, Institut für Baustatik und Baudynamik, Stuttgart, Germany
kato@ibb.uni-stuttgart.de

Kerfriden, Pierre
L.M.T., ENS de Cachan, France
kerfriden@lmt.ens-cachan.fr

Kochmann, Dennis M.
Ruhr-Universität Bochum, Lehrstuhl für Allgemeine Mechanik, Bochum, Germany
dennis.kochmann@rub.de

Kraaijeveld, Famke
Eindhoven University of Technology, Eindhoven, The Netherlands
f.kraaijeveld@tue.nl

Lee, Pilhwa
University of Colorado at Boulder, Department of Mechanical Engineering, Boulder, USA
pilhwa.lee@colorado.edu

Mang, Herbert
Technische Universität Wien, Institut für Mechanik der Werkstoffe und Strukturen, Wien, Austria
herbert.mang@tuwien.ac.at

Markert, Bernd
Universität Stuttgart, Institut für Mechanik (Bauwesen), Stuttgart, Germany
markert@mechbau.uni-stuttgart.de

Maute, Kurt
University of Colorado at Boulder, Department of Aerospace Engineering Sciences, Boulder, USA
maute@colorado.edu

Miehe, Christian
Universität Stuttgart, Institut für Mechanik (Bauwesen), Stuttgart, Germany
cm@mechbau.uni-stuttgart.de

Pahr, Dieter H.
Technische Universität Wien, Institut für Leichtbau und Struktur-Biomechanik, Wien, Austria
pahr@ilsb.tuwien.ac.at

Pesavento, Francesco
Università degli Studi di Padova, Dipartimento di Costruzioni e Trasporti, Padova, Italy
francesco.pesavento@unipd.it

Pichler, Bernhard
Technische Universität Wien, Institut für Mechanik der Werkstoffe und Strukturen, Wien, Austria
bernhard.pichler@tuwien.ac.at

Principe, Javier
Universitat Politécnica de Catalunya, International Center for Numerical Methods in Engineering (CIMNE), Barcelona, Spain
principe@cimne.upc.edu

Ramm, Ekkehard
Universität Stuttgart, Institut für Baustatik und Baudynamik, Stuttgart, Germany
ramm@ibb.uni-stuttgart.de

Rammerstorfer, Franz G.
Technische Universität Wien, Institut für Leichtbau und Struktur-Biomechanik, Wien, Austria
ra@ilsb.tuwien.ac.at

Sanahuja, Julien
Electricité de France (EDF), Department of Materials and Mechanics of Components, Moret-sur-Loing, France
julien.sanahuja@edf.fr

Schrefler, Bernhard A.
Università degli Studi di Padova, Dipartimento di Costruzioni e Trasporti, Padova, Italy
bernhard.schrefler@unipd.it

Scheiner, Stefan
The University of Western Australia, Computer Science and Software Engineering, Crawley, Perth, Western Australia
stefan.scheiner@csse.uwa.edu.au

Scovazzi, Guglielmo
Sandia National Laboratories, Albuquerque, USA
gscovaz@sandia.gov

Suiker, Akke S.J.
Delft University of Technology, Aerospace Engineering, Delft, The Netherlands
a.s.j.suiker@tudelft.nl

van der Zee, Kris
The University of Texas at Austin, Institute for Computational Engineering and Sciences, Austin, USA

van Keulen, Fred
Delft University of Technology, Department of Precision and Microsystems Engineering, Delft, The Netherlands
a.vankeulen@tudelft.nl

Wall, Wolfgang A.
Technische Universität München, Lehrstuhl für Numerische Mechanik, München, Germany
wall@lnm.mw.tum.de

de Wit, Albert J.
Dutch National Aerospace Laboratory (NLR), Amsterdam, The Netherlands
adewit@nlr.nl

Yang, Ronggui
University of Colorado at Boulder, Department of Mechanical Engineering, Boulder, USA
ronggui.yang@colorado.edu

Zäh, Dominic
Universität Stuttgart, Institut für Mechanik (Bauwesen), Stuttgart, Germany
zaeh@mechbau.uni-stuttgart.de

The Micromorphic versus Phase Field Approach to Gradient Plasticity and Damage with Application to Cracking in Metal Single Crystals

Ozgur Aslan and Samuel Forest

MINES ParisTech, Centre des Matériaux, CNRS UMR 7633
BP 87 91003 Evry Cedex, France; samuel.forest@ensmp.fr

Abstract ■■Author, please supply!■■

Key words: ■■Author, please supply!■■

1 Generalized Continua and Material Microstructure

The mechanics of generalized continua represents a way of introducing, in the continuum description of materials, some characteristic length scales associated with their microstructure [24]. Such intrinsic lengths and generalized constitutive equations can be identified in two ways. Direct identification is possible from experimental curves exhibiting clear size effects in plasticity or fracture or from full-field strain measurements of strongly heterogeneous fields [13]. The effective properties of such generalized continua can also be derived from scale transition and homogenization techniques by prescribing appropriate boundary conditions on a representative volume of material with microstructure [5].

The multiplication of generalized continuum model formulations from Cosserat to strain gradient plasticity in literature may leave an impression of disorder and inconsistency. Recent accounts have shown, on the contrary, that unifying presentations of several classes of generalized continuum theories are possible [11, 18]. One of them, called the micromorphic approach, encompasses most theories incorporating additional degrees of freedom from the well-established Cosserat, microstretch and micromorphic continua [9] up to Aifantis and Gurtin strain gradient plasticity theories.

The objective of this chapter is to present this systematic approach for incorporating intrinsic lengths in non-linear continuum mechanical models and to illustrate the efficiency of the method in the case of an anisotropic plasticity and damage model. The so-called *microdamage* model takes the crystallography of plasticity and fracture in metal single crystals.

The micromorphic approach is exposed in Section 2 together with the closely related phase field approach. Differences and similarities between the micromorphic

framework and the phase field approach are pointed out following the general framework provided in [17]. A single crystal plasticity and damage model is explored in Section 3. The finite element implementation and its validation for monotonic crack growth are shown in the two last sections.

The notations used are the same as the ones given in [11]. For the sake of conciseness, the theory and applications are presented within the framework of small deformation.

2 Micromorphic Approach

2.1 Thermomechanics with Additional Degrees of Freedom

One starts from an elastoviscoplasticity model formulation within the framework of the classical Cauchy continuum and classical continuum thermodynamics according to Germain et al. [16] and Maugin [22]. The material behaviour is characterized by the reference sets of degrees of freedom and state variables

$$DOF0 = \{\underline{\boldsymbol{u}}\}, \quad STATE0 = \{\underset{\sim}{\boldsymbol{\varepsilon}}, \quad T, \quad \alpha\} \tag{1}$$

on which the free energy density function ψ may depend. The displacement vector is $\underline{\boldsymbol{u}}$. The strain tensor is denoted by $\underset{\sim}{\boldsymbol{\varepsilon}}$ whereas α represents the whole set of internal variables of arbitrary tensorial order accounting for nonlinear processes at work inside the material volume element, like isotropic and kinematic hardening variables. The absolute temperature is T.

Additional degrees of freedom ${}^{\chi}\phi$ are then introduced in the previous original model. They may be of any tensorial order and of different physical nature (deformation, plasticity or damage variable). The notation ${}^{\chi}$ indicates that these variables eventually represent some microstructural features of the material so that we will call them micromorphic variables or microvariables (microdeformation, microdamage, etc.). The DOF and $STATE$ spaces are extended as follows:

$$DOF = \{\underline{\boldsymbol{u}}, \quad {}^{\chi}\phi\}, \quad STATE = \{\underset{\sim}{\boldsymbol{\varepsilon}}, \quad T, \quad \alpha, \quad {}^{\chi}\phi, \quad \nabla^{\chi}\phi\} \tag{2}$$

Depending on the physical nature of ${}^{\chi}\phi$, it may or may not be a state variable. For instance, if the microvariable is a microrotation as in the Cosserat model, it is not a state variable for objectivity reasons and will appear in $STATE$ only in combination with the macrorotation. In contrast, if the microvariable is a microplastic equivalent strain, as in Aifantis model, it can then explicitly appears in the state space.

The virtual power of internal forces is then extended to the power done by the micromorphic variable and its first gradient:

$$\mathcal{P}^{(i)}(\underline{\boldsymbol{v}}^{\star}, {}^{\chi}\dot{\phi}^{\star}) = -\int_{\mathcal{D}} p^{(i)}(\underline{\boldsymbol{v}}^{\star}, {}^{\chi}\dot{\phi}^{\star})\, dV$$

$$p^{(i)}(\underline{\boldsymbol{v}}^{\star}, {}^{\chi}\dot{\phi}^{\star}) = \underset{\sim}{\boldsymbol{\sigma}} : \nabla \underline{\boldsymbol{v}}^{\star} + a^{\chi}\dot{\phi}^{\star} + \underline{\boldsymbol{b}} \cdot \nabla^{\chi}\dot{\phi}^{\star} \tag{3}$$

where $\mathcal{D}$ is a subdomain of the current configuration Ω of the body. The Cauchy stress is $\underset{\sim}{\boldsymbol{\sigma}}$ and a and $\underline{\boldsymbol{b}}$ are generalized stresses associated with the micromorphic variable and its first gradient. Similarly, the power of contact forces must be extended as follows:

$$\mathcal{P}^{(c)}(\underline{\boldsymbol{v}}^\star, {}^\chi\dot{\phi}^\star) = \int_{\mathcal{D}} p^{(c)}(\underline{\boldsymbol{v}}^\star, {}^\chi\dot{\phi}^\star)\, dV, \quad p^{(c)}(\underline{\boldsymbol{v}}^\star, {}^\chi\dot{\phi}^\star) = \underline{\boldsymbol{t}} \cdot \underline{\boldsymbol{v}}^\star + a^c\, {}^\chi\dot{\phi}^\star \tag{4}$$

where $\underline{\boldsymbol{t}}$ is the traction vector and a^c a generalized traction. For conciseness, we do not extend the power of forces acting at a distance and keep the classical form:

$$\mathcal{P}^{(e)}(\underline{\boldsymbol{v}}^\star, {}^\chi\dot{\phi}^\star) = \int_{\mathcal{D}} p^{(e)}(\underline{\boldsymbol{v}}^\star, {}^\chi\dot{\phi}^\star)\, dV, \quad p^{(e)}(\underline{\boldsymbol{v}}^\star, {}^\chi\dot{\phi}^\star) = \rho \underline{\boldsymbol{f}} \cdot \underline{\boldsymbol{v}}^\star \tag{5}$$

where $\rho \underline{\boldsymbol{f}}$ accounts for given simple body forces. Following Germain [15], given body couples and double forces working with the gradient of the velocity field, could also be introduced in the theory. The generalized principle of virtual power with respect to the velocity and micromorphic variable fields, is presented here in the static case only:

$$\mathcal{P}^{(i)}(\underline{\boldsymbol{v}}^\star, {}^\chi\dot{\phi}) + \mathcal{P}^{(e)}(\underline{\boldsymbol{v}}^\star, {}^\chi\dot{\phi}^\star) + \mathcal{P}^{(c)}(\underline{\boldsymbol{v}}^\star, {}^\chi\dot{\phi}) = 0, \quad \forall \mathcal{D} \subset \Omega, \quad \forall \underline{\boldsymbol{v}}^\star, {}^\chi\dot{\phi} \tag{6}$$

The method of virtual power according to Maugin [21] is used then to derive the standard local balance of momentum equation:

$$\operatorname{div} \underset{\sim}{\boldsymbol{\sigma}} + \rho \underline{\boldsymbol{f}} = 0, \quad \forall \underline{\boldsymbol{x}} \in \Omega \tag{7}$$

and the generalized balance of micromorphic momentum equation:

$$\operatorname{div} \underline{\boldsymbol{b}} - a = 0, \quad \forall \underline{\boldsymbol{x}} \in \Omega \tag{8}$$

The method also delivers the associated boundary conditions for the simple and generalized tractions:

$$\underline{\boldsymbol{t}} = \underset{\sim}{\boldsymbol{\sigma}}.\underline{\boldsymbol{n}}, \quad a^c = \underline{\boldsymbol{b}}.\underline{\boldsymbol{n}}, \quad \forall \underline{\boldsymbol{x}} \in \partial\mathcal{D} \tag{9}$$

The local balance of energy is also enhanced by the generalized micromorphic power already included in the power of internal forces (3):

$$\rho\dot{\epsilon} = p^{(i)} - \operatorname{div} \underline{\boldsymbol{q}} + \rho r \tag{10}$$

where ϵ is the specific internal energy, $\underline{\boldsymbol{q}}$ the heat flux vector and r denotes external heat sources. The entropy principle takes the usual local form:

$$-\rho(\dot{\psi} + \eta\dot{T}) + p^{(i)} - \frac{\underline{\boldsymbol{q}}}{T}.\nabla T \geq 0 \tag{11}$$

where it is assumed that the entropy production vector is still equal to the heat vector divided by temperature, as in classical thermomechanics according to Coleman and Noll [6]. Again, the enhancement of the theory goes through the enriched power

density of internal forces (3). The entropy principle is exploited according to classical continuum thermodynamics to derive the state laws. At this stage it is necessary to be more specific on the dependence of the state functions $\psi, \eta, \underset{\sim}{\boldsymbol{\sigma}}, a, \underline{\boldsymbol{b}}$ on state variables and to distinguish between dissipative and non-dissipative mechanisms. The introduction of dissipative mechanisms may require an increase in the number of state variables. These different situations are considered in the following subsections.

2.2 Non-Dissipative Contribution of Generalized Stresses and Micromorphic Model

Dissipative events are assumed here to enter the model only via the classical mechanical part. Total strain is split into elastic and plastic parts:

$$\underset{\sim}{\boldsymbol{\varepsilon}} = \underset{\sim}{\boldsymbol{\varepsilon}}^e + \underset{\sim}{\boldsymbol{\varepsilon}}^p \tag{12}$$

The following constitutive functional dependencies are then introduced:

$$\psi = \hat{\psi}(\underset{\sim}{\boldsymbol{\varepsilon}}^e, T, \alpha, {}^{\chi}\phi, \nabla^{\chi}\phi), \quad \underset{\sim}{\boldsymbol{\sigma}} = \hat{\underset{\sim}{\boldsymbol{\sigma}}}(\underset{\sim}{\boldsymbol{\varepsilon}}^e, T, \alpha, {}^{\chi}\phi, \nabla^{\chi}\phi), \quad \eta = \hat{\eta}(\underset{\sim}{\boldsymbol{\varepsilon}}^e, T, \alpha, {}^{\chi}\phi, \nabla^{\chi}\phi)$$

$$a = \hat{a}(\underset{\sim}{\boldsymbol{\varepsilon}}^e, T, \alpha, {}^{\chi}\phi, \nabla^{\chi}\phi), \quad \underline{\boldsymbol{b}} = \hat{\underline{\boldsymbol{b}}}(\underset{\sim}{\boldsymbol{\varepsilon}}^e, T, \alpha, {}^{\chi}\phi, \nabla^{\chi}\phi) \tag{13}$$

The entropy inequality (11) can be expanded as

$$\left(\underset{\sim}{\boldsymbol{\sigma}} - \rho\frac{\partial\hat{\psi}}{\partial\underset{\sim}{\boldsymbol{\varepsilon}}^e}\right) : \dot{\underset{\sim}{\boldsymbol{\varepsilon}}}^e + \rho\left(\eta + \frac{\partial\hat{\psi}}{\partial T}\right)\dot{T} + \left(a - \rho\frac{\partial\hat{\psi}}{\partial\,{}^{\chi}\phi}\right){}^{\chi}\dot{\phi} + \left(\underline{\boldsymbol{b}} - \rho\frac{\partial\hat{\psi}}{\partial\nabla\,{}^{\chi}\phi}\right)\cdot\nabla\,{}^{\chi}\dot{\phi}$$

$$+\underset{\sim}{\boldsymbol{\sigma}} : \dot{\underset{\sim}{\boldsymbol{\varepsilon}}}^p - \rho\frac{\partial\hat{\psi}}{\partial\alpha}\dot{\alpha} - \frac{\underline{\boldsymbol{q}}}{T}\cdot\nabla T \geq 0 \tag{14}$$

Assuming that no dissipation is associated with the four first terms of the previous inequality, the following state laws are found:

$$\underset{\sim}{\boldsymbol{\sigma}} = \rho\frac{\partial\hat{\psi}}{\partial\underset{\sim}{\boldsymbol{\varepsilon}}^e}, \quad \eta = -\frac{\partial\hat{\psi}}{\partial T}, \quad X = \rho\frac{\partial\hat{\psi}}{\partial\alpha} \tag{15}$$

$$a = \rho\frac{\partial\hat{\psi}}{\partial\,{}^{\chi}\phi}, \quad \underline{\boldsymbol{b}} = \rho\frac{\partial\hat{\psi}}{\partial\nabla\,{}^{\chi}\phi} \tag{16}$$

and the residual dissipation is

$$D^{res} = W^p - X\dot{\alpha} - \frac{\underline{\boldsymbol{q}}}{T}.\nabla T \geq 0 \tag{17}$$

where W^p represents the (visco-)plastic power and X the thermodynamic force associated with the internal variable α. The existence of a convex dissipation potential, $\Omega(\underset{\sim}{\boldsymbol{\sigma}}, X)$ depending on the thermodynamic forces can then be assumed from which the evolution rules for internal variables are derived, that identically fulfill the entropy inequality, as usually done in classical continuum thermomechanics [16]:

$$\dot{\underset{\sim}{\boldsymbol{\varepsilon}}}^p = \frac{\partial\Omega}{\partial\underset{\sim}{\boldsymbol{\sigma}}}, \quad \dot{\alpha} = \frac{\partial\Omega}{\partial X} \tag{18}$$

Micromorphic Model

After presenting the general approach, we readily give the most simple example which provides a direct connection to several existing generalized continuum models. We consider first cases where ϕ and ${}^{\chi}\phi$ are observer invariant quantities. The free energy density function ψ is chosen as a function of the generalized relative strain variable e defined as:

$$e = \phi - {}^{\chi}\phi \tag{19}$$

thus introducing a coupling between macro and micromorphic variables. Assuming isotropic material behavior for brevity, the additional contributions to the free energy can be taken as quadratic functions of e and $\boldsymbol{\nabla}^{\chi}\phi$:

$$\psi(\underset{\sim}{\boldsymbol{\varepsilon}}, T, \alpha, {}^{\chi}\phi, \boldsymbol{\nabla}^{\chi}\phi) = \psi^{(1)}(\underset{\sim}{\boldsymbol{\varepsilon}}, T, \alpha) + \psi^{(2)}(e = \phi - {}^{\chi}\phi, \boldsymbol{\nabla}^{\chi}\phi, T), \quad \text{with} \tag{20}$$

$$\rho\psi^{(2)}(e, \boldsymbol{\nabla}^{\chi}\phi, T) = \frac{1}{2}H_{\chi}(\phi - {}^{\chi}\phi)^2 + \frac{1}{2}A\boldsymbol{\nabla}^{\chi}\phi \cdot \boldsymbol{\nabla}^{\chi}\phi \tag{21}$$

After inserting the state laws (16)

$$a = \rho\frac{\partial\psi}{\partial^{\chi}\phi} = -H_{\chi}(\phi - {}^{\chi}\phi), \quad \underline{\boldsymbol{b}} = \rho\frac{\partial\psi}{\partial\boldsymbol{\nabla}^{\chi}\phi} = A\boldsymbol{\nabla}^{\chi}\phi \tag{22}$$

into the additional balance equation (8), the following partial differential equation is obtained, at least for a homogeneous material under isothermal conditions:

$$\phi = {}^{\chi}\phi - \frac{A}{H_{\chi}}\Delta^{\chi}\phi \tag{23}$$

where Δ is the Laplace operator. This type of equation is encountered at several places in the mechanics of generalized continua especially in the linear micromorphic theory [7, 9, 23] and in the so-called implicit gradient theory of plasticity and damage [8, 25, 26]. Note however that this equation corresponds to a special quadratic potential and represents the simplest micromorphic extension of the classical theory. It involves a characteristic length scale defined by

$$l_c^2 = \frac{A}{H_{\chi}} \tag{24}$$

This length is real for positive values of the ratio A/H_{χ}. The additional material parameters H_X and A are assumed to be positive in this work. This does not exclude a softening material behaviour that can be induced by the proper evolution of the internal variables (including $\phi = \alpha$ itself).

2.3 Viscous Generalized Stress and Phase Field Model

Generalized stresses can also be associated with dissipation by introducing the viscous part a^v of a:

$$\underset{\sim}{\boldsymbol{\varepsilon}} = \underset{\sim}{\boldsymbol{\varepsilon}}^e + \underset{\sim}{\boldsymbol{\varepsilon}}^p, \quad a = a^e + a^v \tag{25}$$

The entropy inequality (11) now becomes

$$\left(\underset{\sim}{\boldsymbol{\sigma}} - \rho\frac{\partial\hat{\psi}}{\partial\underset{\sim}{\boldsymbol{\varepsilon}}^e}\right) : \dot{\underset{\sim}{\boldsymbol{\varepsilon}}}^e + \rho\left(\eta + \frac{\partial\hat{\psi}}{\partial T}\right)\dot{T} + \left(a^e - \rho\frac{\partial\hat{\psi}}{\partial\,{}^{\chi}\phi}\right){}^{\chi}\dot{\phi} + \left(\underline{\boldsymbol{b}} - \rho\frac{\partial\hat{\psi}}{\partial\nabla\,{}^{\chi}\phi}\right)\cdot\nabla\,{}^{\chi}\dot{\phi}$$

$$+\underset{\sim}{\boldsymbol{\sigma}} : \dot{\underset{\sim}{\boldsymbol{\varepsilon}}}^p - \rho\frac{\partial\hat{\psi}}{\partial\alpha}\dot{\alpha} + a^v\,{}^{\chi}\dot{\phi} - \frac{\underline{\boldsymbol{q}}}{T}\cdot\nabla T \geq 0 \tag{26}$$

Assuming that no dissipation is associated with the four first terms of the previous inequality, the following state laws are found:

$$\underset{\sim}{\boldsymbol{\sigma}} = \rho\frac{\partial\hat{\psi}}{\partial\underset{\sim}{\boldsymbol{\varepsilon}}^e}, \quad \eta = -\frac{\partial\hat{\psi}}{\partial T}, \quad X = \rho\frac{\partial\hat{\psi}}{\partial\alpha} \tag{27}$$

$$a^e = \rho\frac{\partial\hat{\psi}}{\partial\,{}^{\chi}\phi}, \quad \underline{\boldsymbol{b}} = \rho\frac{\partial\hat{\psi}}{\partial\nabla\,{}^{\chi}\phi} \tag{28}$$

and the residual dissipation is

$$D^{res} = \underset{\sim}{\boldsymbol{\sigma}} : \dot{\underset{\sim}{\boldsymbol{\varepsilon}}}^p - X\dot{\alpha} + a^v\,{}^{\chi}\dot{\phi} - \frac{\underline{\boldsymbol{q}}}{T}\cdot\nabla T \geq 0 \tag{29}$$

Evolution rules for viscoplastic strain, internal variables, and the additional degrees of freedom can be derived from a dissipation potential $\Omega(\underset{\sim}{\boldsymbol{\sigma}}, X, a^v)$:

$$\dot{\underset{\sim}{\boldsymbol{\varepsilon}}}^p = \frac{\partial\Omega}{\partial\underset{\sim}{\boldsymbol{\sigma}}}, \quad \dot{\alpha} = \frac{\partial\Omega}{\partial X}, \quad {}^{\chi}\dot{\phi} = \frac{\partial\Omega}{\partial a^v} \tag{30}$$

Convexity of the dissipation potential then ensures positivity of dissipation rate for any process.

Note that no dissipative part has been assigned to the generalized stress $\underline{\boldsymbol{b}}$ since then exploitation of second principle does not seem to be straightforward. Instead, the total gradient $\nabla\,{}^{\chi}\phi$ can be split into elastic and plastic parts, as it will be done in Section 2.4.

Phase Field Model

The dissipation potential can be decomposed into the various contributions due to all thermodynamic forces. Let us assume for instance that the contribution of the viscous generalized stress a^v is quadratic:

$$\Omega(\underset{\sim}{\boldsymbol{\sigma}}, X, a^v) = \Omega_1(\underset{\sim}{\boldsymbol{\sigma}}, X) + \Omega_2(a^v), \quad \Omega_2(a^v) = \frac{1}{2\beta}a^{v2} \tag{31}$$

The use of the flow rule (30) and of the additional balance equation (8) then leads to

$$\beta\,{}^{\chi}\dot{\phi} = a^{v} = a - a^{e} = a - \rho\frac{\partial\hat{\psi}}{\partial\,{}^{\chi}\phi} = \operatorname{div}\rho\frac{\partial\hat{\psi}}{\partial\nabla\,{}^{\chi}\phi} - \rho\frac{\partial\hat{\psi}}{\partial\,{}^{\chi}\phi} \tag{32}$$

One recognizes the Landau–Ginzburg equation that arises in phase field theories. The previous derivation of Landau–Ginzburg equation is due to Mühlhaus [1] and Peerlings et al. [17]. The coupling with mechanics is straightforward according to this procedure and more general dissipative mechanics can be put forward.

2.4 Elasto-Plastic Decomposition of Generalized Strains

Instead of the previous decomposition of generalized stresses, the introduction of additional dissipative mechanisms can rely on the split of all strain measures into elastic and plastic parts:

$$\underset{\sim}{\boldsymbol{\varepsilon}} = \underset{\sim}{\boldsymbol{\varepsilon}}^{e} + \underset{\sim}{\boldsymbol{\varepsilon}}^{p}, \quad {}^{\chi}\phi = {}^{\chi}\phi^{e} + {}^{\chi}\phi^{p}, \quad \underline{\boldsymbol{\kappa}} = \nabla\,{}^{\chi}\phi = \underline{\boldsymbol{\kappa}}^{\,e} + \underline{\boldsymbol{\kappa}}^{\,p} \tag{33}$$

The objectivity of ${}^{\chi}\phi$ is required for such a unique decomposition to be defined. We do not require here that

$$\underline{\boldsymbol{\kappa}}^{\,e} = \nabla^{\chi}\phi^{e}, \quad \underline{\boldsymbol{\kappa}}^{\,p} = \nabla^{\chi}\phi^{p} \tag{34}$$

although such a model also is possible, as illustrated by the *gradient of strain theory* put forward in [12]. The Clausius–Duhem inequality then writes

$$\left(\underset{\sim}{\boldsymbol{\sigma}} - \rho\frac{\partial\hat{\psi}}{\partial\underset{\sim}{\boldsymbol{\varepsilon}}^{e}}\right) : \dot{\underset{\sim}{\boldsymbol{\varepsilon}}}^{e} + \rho\left(\eta + \frac{\partial\hat{\psi}}{\partial T}\right)\dot{T} + \left(a - \rho\frac{\partial\hat{\psi}}{\partial\,{}^{\chi}\phi}\right){}^{\chi}\dot{\phi}^{e} + \left(\underline{\boldsymbol{b}} - \rho\frac{\partial\hat{\psi}}{\partial\nabla\,{}^{\chi}\phi}\right)\cdot\dot{\underline{\boldsymbol{\kappa}}}^{\,e}$$

$$+\underset{\sim}{\boldsymbol{\sigma}} : \dot{\underset{\sim}{\boldsymbol{\varepsilon}}}^{p} - \rho\frac{\partial\hat{\psi}}{\partial\alpha}\dot{\alpha} + a\,{}^{\chi}\dot{\phi}^{p} + \underline{\boldsymbol{b}}\cdot\dot{\underline{\boldsymbol{\kappa}}}^{\,p} - \frac{\underline{\boldsymbol{q}}}{T}\cdot\nabla T \geq 0 \tag{35}$$

Assuming that no dissipation is associated with the four first terms of the previous inequality, the following state laws are found:

$$\underset{\sim}{\boldsymbol{\sigma}} = \rho\frac{\partial\hat{\psi}}{\partial\underset{\sim}{\boldsymbol{\varepsilon}}^{e}}, \quad \eta = -\frac{\partial\hat{\psi}}{\partial T}, \quad X = \rho\frac{\partial\hat{\psi}}{\partial\alpha} \tag{36}$$

$$a = \rho\frac{\partial\hat{\psi}}{\partial\,{}^{\chi}\phi^{e}}, \quad \underline{\boldsymbol{b}} = \rho\frac{\partial\hat{\psi}}{\partial\underline{\boldsymbol{\kappa}}^{\,e}} \tag{37}$$

and the residual dissipation is

$$D^{res} = \underset{\sim}{\boldsymbol{\sigma}} : \dot{\underset{\sim}{\boldsymbol{\varepsilon}}}^{p} - X\dot{\alpha} + a\,{}^{\chi}\dot{\phi}^{p} + \underline{\boldsymbol{b}}\cdot\dot{\underline{\boldsymbol{\kappa}}}^{\,p} - \frac{\underline{\boldsymbol{q}}}{T}\cdot\nabla T \geq 0 \tag{38}$$

Evolution rules for viscoplastic strain, internal variables, and the additional degrees of freedom can be derived from a dissipation potential $\Omega(\underset{\sim}{\boldsymbol{\sigma}}, X, a, \underline{\boldsymbol{b}})$:

$$\dot{\underset{\sim}{\boldsymbol{\varepsilon}}}^{p} = \frac{\partial\Omega}{\partial\underset{\sim}{\boldsymbol{\sigma}}}, \quad \dot{\alpha} = \frac{\partial\Omega}{\partial X}, \quad {}^{\chi}\dot{\phi}^{p} = \frac{\partial\Omega}{\partial a}, \quad \dot{\underline{\boldsymbol{\kappa}}}^{\,p} = \frac{\partial\Omega}{\partial\underline{\boldsymbol{b}}} \tag{39}$$

As a result of the additional balance equation (8) combined with the previous state laws, the type of derived partial differential equation can be made more specific by adopting a quadratic free energy potential for $\underline{\boldsymbol{b}}$ (modulus A) and a quadratic dissipation potential with respect to a (parameter β). We obtain:

$$\beta^{\chi}\dot{\phi} = a + \beta^{\chi}\dot{\phi}^{e} = \operatorname{div} A\underline{\boldsymbol{\kappa}} - \operatorname{div} A\underline{\boldsymbol{\kappa}}^{p} + \beta^{\chi}\dot{\phi}^{e} \tag{40}$$

Decompositions of stresses and strains can also be mixed, for instance in the following way:

$$\underset{\sim}{\boldsymbol{\varepsilon}} = \underset{\sim}{\boldsymbol{\varepsilon}}^{e} + \underset{\sim}{\boldsymbol{\varepsilon}}^{p}, \quad a = a^{e} + a^{v}, \quad \underline{\boldsymbol{\kappa}} = \nabla^{\chi}\phi = \underline{\boldsymbol{\kappa}}^{e} + \underline{\boldsymbol{\kappa}}^{p} \tag{41}$$

based on which a constitutive theory can be built.

3 Continuum Damage Model for Single Crystals and Its Regularization

We present here a constitutive model for damaging viscoplastic single crystal behaviour aiming at simulating crack initiation and propagation. The micromorphic approach is then applied to this model in order to obtain a regularized continuum damage formulation with a view to simulating mesh-independent crack propagation in single crystals.

3.1 Constitutive Equations

In the proposed crystal plasticity model taken from [20], viscoplasticity and damage are coupled by introducing an additional damage strain variable $\underset{\sim}{\boldsymbol{\varepsilon}}^{d}$, into the strain rate partition equation:

$$\dot{\underset{\sim}{\boldsymbol{\varepsilon}}} = \dot{\underset{\sim}{\boldsymbol{\varepsilon}}}^{e} + \dot{\underset{\sim}{\boldsymbol{\varepsilon}}}^{p} + \dot{\underset{\sim}{\boldsymbol{\varepsilon}}}^{d} \tag{42}$$

where $\dot{\underset{\sim}{\boldsymbol{\varepsilon}}}^{e}$ and $\dot{\underset{\sim}{\boldsymbol{\varepsilon}}}^{p}$ are the elastic and the plastic strain rates, respectively. The flow rule for plastic part is written at the slip system level by means of the orientation tensor $\underset{\sim}{\boldsymbol{m}}^{s}$:

$$\underset{\sim}{\boldsymbol{m}}^{s} = \frac{1}{2}(\underline{\boldsymbol{n}}^{s} \otimes \underline{\boldsymbol{l}}^{s} + \underline{\boldsymbol{l}}^{s} \otimes \underline{\boldsymbol{n}}^{s}) \tag{43}$$

where $\underline{\boldsymbol{n}}^{s}$ is the normal to the plane of slip system s and $\underline{\boldsymbol{l}}^{s}$ stands for the corresponding slip direction. Then, plastic strain rate reads:

$$\dot{\underset{\sim}{\boldsymbol{\varepsilon}}}^{p} = \sum_{s=1}^{N_{slip}} \dot{\gamma}^{s}\underset{\sim}{\boldsymbol{m}}^{s} \tag{44}$$

The flow rule on slip system s is a classical Norton rule with threshold.

$$\dot{\gamma}^{s} = \left\langle \frac{|\tau^{s} - x^{s}| - r^{s}}{K} \right\rangle^{n} sign(\tau^{s} - x^{s}) \tag{45}$$

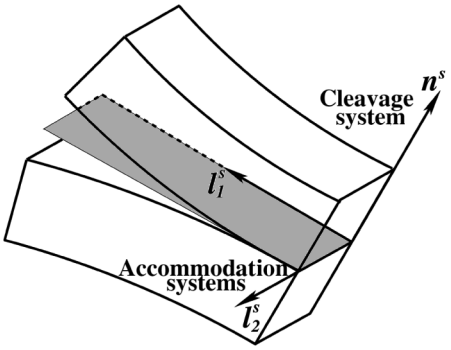

Fig. 1. Illustration of the cleavage and two accommodation systems to be associated to the crystallographic planes.

where r^s and x^s are the variables for isotropic and kinematic hardening respectively and K and n are material parameters to be identified from experimental curves.

Material separation is assumed to take place w.r.t. specific crystallographic planes, like cleavage planes in single crystals. The word *cleavage* is written in a more general sense that its original meaning in physical metallurgy associated with brittle fracture of non-f.c.c. crystals. In the continuum mechanical model, *cleavage* means cracking along a specific crystallographic plane as it is often observed in low cycle fatigue of f.c.c. crystals like single crystal nickel-base superalloys. The damage strain $\underset{\sim}{\dot{\boldsymbol{\varepsilon}}}^d$ is decomposed in the following crystallographic contributions:

$$\underset{\sim}{\dot{\boldsymbol{\varepsilon}}}^d = \sum_{s=1}^{N_{damage}} \dot{\delta}_c^s \underline{\boldsymbol{n}}_d^s \otimes \underline{\boldsymbol{n}}_d^s + \dot{\delta}_1^s \underline{\boldsymbol{n}}_d^s \overset{sym}{\otimes} \underline{\boldsymbol{l}}_{d_1}^s + \dot{\delta}_2^s \underline{\boldsymbol{n}}_d^s \overset{sym}{\otimes} \underline{\boldsymbol{l}}_{d_2}^s \tag{46}$$

where $\dot{\delta}^s$, $\dot{\delta}_1^s$ and $\dot{\delta}_2^s$ are the strain rates for mode I, mode II and mode III crack growth, respectively and N_{damage}^d stands for the number of damage planes which are fixed crystallographic planes depending on the crystal structure. Cleavage damage is represented by the opening δ^s of crystallographic cleavage planes with the normal vector $\underline{\boldsymbol{n}}^s$. Additional damage systems must be introduced for the in-plane accommodation along orthogonal directions $\underline{\boldsymbol{l}}_1^s$ and $\underline{\boldsymbol{l}}_2^s$, once cleavage has started (Figure 1). Three damage criteria are associated to one cleavage and two accommodation systems:

$$f_c^s = \left| \underline{\boldsymbol{n}}_d^s \cdot \underset{\sim}{\boldsymbol{\sigma}} \cdot \underline{\boldsymbol{n}}_d^s \right| - Y_c^s \tag{47}$$

$$f_i^s = \left| \underline{\boldsymbol{n}}_d^s \cdot \underset{\sim}{\boldsymbol{\sigma}} \cdot \underline{\boldsymbol{l}}_{d_i}^s \right| - Y_i^s \quad (i = 1, 2) \tag{48}$$

The critical normal stress Y^s for damage decreases as δ increases:

$$Y_c^s = Y_0^s + H\delta_c^s\,, \quad Y_i^s = Y_0^s + H\delta_i^s \tag{49}$$

where Y_0^s is the initial damage stress (usually coupled to plasticity) and H is a negative modulus which controls material softening due to damage. Finally, evolution of damage is given by the following equations:

$$\dot{\delta}_c^s = \left\langle \frac{f_c^s}{K_d} \right\rangle^{n_d} \text{sign}\left(\underline{\boldsymbol{n}}_d^s \cdot \underset{\sim}{\boldsymbol{\sigma}} \cdot \underline{\boldsymbol{n}}_d^s\right) \tag{50}$$

$$\dot{\delta}_i^s = \left\langle \frac{f_i^s}{K_d} \right\rangle^{n_d} \text{sign}\left(\underline{\boldsymbol{n}}_d^s \cdot \underset{\sim}{\boldsymbol{\sigma}} \cdot \underline{\boldsymbol{l}}_{d_i}^s\right) \tag{51}$$

where K_d and n_d are material parameters.

These equations hold for all conditions except when the crack is closed ($\delta_c^s < 0$) and compressive forces are applied ($\underline{\boldsymbol{n}}_d^s \cdot \underset{\sim}{\boldsymbol{\sigma}} \cdot \underline{\boldsymbol{n}}_d^s < 0$). In this case, damage evolution stops ($\dot{\delta}_c^s = \dot{\delta}_i^s = 0$), corresponding to the unilateral damage conditions.

Note that the damage variables δ introduced in the model differ from the usual corresponding variables of standard continuum damage mechanics that vary from 0 to 1. In contrast, the δs are strain-like quantities that can ever increase.

Coupling between plasticity and damage is generated through initial damage stress Y_0 in (49) which is controlled by cumulative slip variable γ_{cum}:

$$\dot{\gamma}_{cum} = \sum_{s=1}^{N_{slips}} |\dot{\gamma}^s| \tag{52}$$

Then, Y_0 takes the form:

$$Y_0^s = \sigma_n^c \, e^{-d\gamma_{cum}} + \sigma_{ult} \tag{53}$$

This formulation suggests an exponential decaying regime from a preferably high initial cleavage stress value σ_n^c, to an ultimate stress, σ_{ult} which is close to but not equal to zero for numerical reasons and d is a material constant.

This model, complemented by the suitable constitutive equations for viscoplastic strain, has been used for the simulation of crack growth under complex cyclic loading at high temperature [19]. Significant mesh dependency of results was found [20].

In the present work, the model is further developed by switching from classical to microdamage continuum in order to assess the regularization capabilities of a higher order theory. The coupling of the model with microdamage theory is achieved by introducing a cumulative damage variable calculated from the damage systems and a new threshold function $Y_0(\delta, \gamma_{cum})$:

$$\dot{\delta}_{cum} = \sum_{s=1}^{N_{planes}} \dot{\delta}^s \ , \ \text{where} \ \dot{\delta}^s = |\dot{\delta}_c^s| + |\dot{\delta}_1^s| + |\dot{\delta}_2^s| \tag{54}$$

$$Y_0 = \sigma_n^c \, e^{-d\gamma_{cum} - H\delta_{cum}} + \sigma_{ult} \tag{55}$$

3.2 Microdamage Continuum

The micromorphic medium introduced by Eringen and Suhubi [10] possesses a full microdeformation field $\underset{\sim}{\boldsymbol{\chi}}$, in addition to the classical displacement field $\underline{\boldsymbol{u}}$. Containing additional degrees of freedom and balance equations, the micromorphic continuum approach can be considered as the main framework for most generalized

continuum models [11]. Alternative micromorphic variables other than the full strain tensor can be chosen [2, 11]. The strain gradient effect can for instance be limited to the damage strain $\underset{\sim}{\boldsymbol{\varepsilon}}^d$ gradient and more specifically to the damage variable δ_{cum} introduced in the previous model and noted here δ for conciseness.

In microdamage theory, the introduced microvariable is a scalar microdamage parameter ${}^{\chi}\delta$:

$$DOF = \{\underline{\boldsymbol{u}},\ {}^{\chi}\delta\} \qquad STRAIN = \{\underset{\sim}{\boldsymbol{\varepsilon}},\ {}^{\chi}\delta, \nabla\, {}^{\chi}\delta\} \tag{56}$$

The power of internal forces is extended as

$$p^{(i)} = \underset{\sim}{\boldsymbol{\sigma}} : \dot{\underset{\sim}{\boldsymbol{\varepsilon}}} + a\, {}^{\chi}\dot{\delta} + \underline{\boldsymbol{b}} . \nabla\, {}^{\chi}\dot{\delta} \tag{57}$$

where generalized stresses a, $\underline{\boldsymbol{b}}$ have been introduced. The generalized balance equations are:

$$\operatorname{div} \underset{\sim}{\boldsymbol{\sigma}} = 0, \quad a = \operatorname{div} \underline{\boldsymbol{b}} \tag{58}$$

The free energy density is taken as a quadratic potential in the elastic strain, damage δ, relative damage $\delta - {}^{\chi}\delta$ and microdamage gradient $\nabla {}^{\chi}\delta$:

$$\rho\psi = \frac{1}{2}\underset{\sim}{\boldsymbol{\varepsilon}}^e : \underset{\sim}{\underset{\sim}{\boldsymbol{c}}} : \underset{\sim}{\boldsymbol{\varepsilon}}^e + \frac{1}{2}\sum_{s=1}^{N_{damage}} H\delta_s^2 + \frac{1}{2}\,{}^{\chi}H(\delta - {}^{\chi}\delta)^2 + \frac{1}{2}A\nabla\, {}^{\chi}\delta \cdot \nabla\, {}^{\chi}\delta \tag{59}$$

where H, ${}^{\chi}H$ and A are scalar material constants. Then, the elastic response of the material becomes

$$\underset{\sim}{\boldsymbol{\sigma}} = \rho\frac{\partial\psi}{\partial \underset{\sim}{\boldsymbol{\varepsilon}}^e} = \underset{\sim}{\underset{\sim}{\boldsymbol{c}}} : \underset{\sim}{\boldsymbol{\varepsilon}}^e \tag{60}$$

The generalized stresses read

$$a = \rho\frac{\partial\psi}{\partial\, {}^{\chi}\delta} = -\,{}^{\chi}H(\delta - {}^{\chi}\delta)\,, \quad \underline{\boldsymbol{b}} = A\nabla\, {}^{\chi}\delta \tag{61}$$

and the driving force for damage can be derived as

$$Y^s = \rho\frac{\partial\psi}{\partial\delta^s} = H\delta^s + {}^{\chi}H(\delta^s - {}^{\chi}\delta) \tag{62}$$

The damage criterion is now

$$f^s = \left|\underline{\boldsymbol{n}}^s \cdot \underset{\sim}{\boldsymbol{\sigma}} \cdot \underline{\boldsymbol{n}}^s\right| - Y_0 - Y^s = 0 \tag{63}$$

Substituting the linear constitutive equations for generalized stresses into the additional balance equation (58), assuming homogeneous material properties, leads to the following partial differential equation for the microdamage:

$${}^{\chi}\delta - \frac{A}{{}^{\chi}H}\Delta\, {}^{\chi}\delta = \delta \tag{64}$$

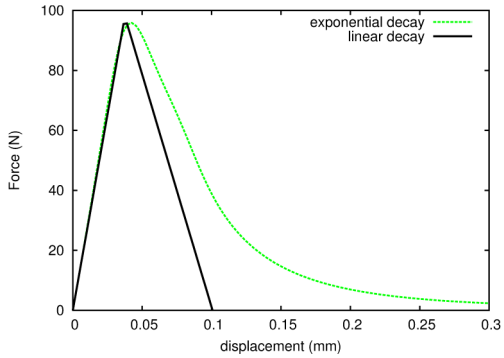

Fig. 2. Comparison between force vs. displacement diagram of a 1D softening rod for linear and exponential decay.

where the macrodamage δ acts as a source term. Exactly this type of Helmholtz equation has been postulated in the so-called implicit gradient theory of plasticity and damage [8, 14, 25, 26], where the microvariables are called non local variables and where the generalized stresses a and $\underline{\boldsymbol{b}}$ are not explicitly introduced (see [7, 11] for the analogy between this latter approach and the micromorphic theory).

The solution of the problem of failure of a 1D bar in tension/compression was treated in [2]. The characteristic size of the damage zone was shown to be controlled by the characteristic length corresponding to the inverse of

$$\omega = \sqrt{|H\, \chi H / A(H + \chi H)|} \tag{65}$$

In comparison with the standard strain gradient approaches [14, 25], microdamage theory eliminates the final fracture problem without any modification to the damage function, since there exists no direct coupling between the force stress $\underset{\sim}{\boldsymbol{\sigma}}$ and the generalized stresses, a and $\underline{\boldsymbol{b}}$. For a better representation of a cracked element, we suggest an exponential drop both for damage threshold Y_0 and the modulus A, since the element should become unable to store energy due to the generalized stresses when broken (see Figure 2):

$$Y_0 = \sigma_n^c\, e^{-H\delta} + \sigma_{ult}\ , \quad \underline{\boldsymbol{b}} = A e^{-H\delta} \nabla\, \chi \delta \tag{66}$$

4 Finite Element Implementation

4.1 Variational Formulation and Discretization

The variational formulation of the microdamage approach can be derived directly from the principle of virtual power (57):

$$\int_\Omega p^{(i)} dV + \int_{\partial\Omega} p^{(c)} dS = 0 \tag{67}$$

$$\int_\Omega (\underset{\sim}{\boldsymbol{\sigma}} : \dot{\underset{\sim}{\boldsymbol{\varepsilon}}} + a\,{}^{\chi}\dot{\delta} + \underline{\boldsymbol{b}}.\nabla\,{}^{\chi}\dot{\delta})dV + \int_{\partial\Omega} (\underline{\boldsymbol{t}}.\underline{\dot{\boldsymbol{u}}} + a\,{}^{\chi}\dot{\delta})dS = 0 \tag{68}$$

Finite element discretization of the displacement field $\underline{\boldsymbol{u}}$ and the microdamage field ${}^{\chi}\delta$ takes the following form:

$$u = N_u d_u, \quad \nabla u = B_u d_u, \quad {}^{\chi}\delta = N_\delta d_\delta, \quad \nabla {}^{\chi}\delta = B_\delta d_\delta \tag{69}$$

where d_u and d_δ are the nodal degrees of freedom. N_u and N_δ represent the shape functions and B_u and B_δ stand for their partial derivatives with respect to the coordinates. In this work we use isoparametric quadratic elements for both types of degrees of freedom.

Finally, the discretized equilibrium equations read:

$$\int_\Omega B_u^T \underset{\sim}{\boldsymbol{\sigma}} dV = \int_\Omega {N_u}^T \underline{\boldsymbol{f}}\, dV + \int_\Gamma {N_u}^T \underline{\boldsymbol{t}}\, dS \tag{70}$$

$$\int_\Omega ({N_\delta}^T a + {B_\delta}^T \underline{\boldsymbol{b}})dV = \int_\Gamma {N_\delta}^T a_c dS \tag{71}$$

4.2 Implicit Incremental Formulation

A fully implicit Newton–Raphson incremental formulation is developed for solving (70, 71). The corresponding time discretization is now introduced. Using the known values of the state variables $\underset{\sim}{\boldsymbol{\varepsilon}}^e(t)$, $\upsilon^s(t)$ (integrated from $\dot{\upsilon}^s = |\dot{\gamma}^s|$),$\delta^s_{c,i}(t)$, $\delta^s_{cum}(t)$ for the current time step, the values at $t + \Delta t$ are estimated by a straight forward linearization procedure.

$$\underset{\sim}{\boldsymbol{\varepsilon}}^e(t + \Delta t) = \underbrace{\Delta t\, \dot{\underset{\sim}{\boldsymbol{\varepsilon}}}^e(t + \Delta t)}_{\Delta \underset{\sim}{\boldsymbol{\varepsilon}}^e} + \underset{\sim}{\boldsymbol{\varepsilon}}^e(t) \tag{72}$$

$$\upsilon^s(t + \Delta t) = \Delta t\, \dot{\upsilon}^s(t + \Delta t) + \upsilon^s(t) \tag{73}$$

$$\delta^s_{c,i}(t + \Delta t) = \Delta t\, \dot{\delta}^s_{c,i}(t + \Delta t) + \delta^s_{c,i}(t) \tag{74}$$

$$\delta^s_{cum}(t + \Delta t) = \Delta t\, \dot{\delta}^s_{cum}(t + \Delta t) + \delta^s_{cum}(t) \tag{75}$$

The model is implemented into the FE code ZeBuLoN [4], using a θ-method for the local integration. In order to calculate the state variable increments, the residuals and their Jacobian are written as follows:

$$R_{\underset{\sim}{\boldsymbol{\varepsilon}}^e} = \Delta \underset{\sim}{\boldsymbol{\varepsilon}}^e + \Delta \underset{\sim}{\boldsymbol{\varepsilon}}^p + \Delta \underset{\sim}{\boldsymbol{\varepsilon}}^d - \Delta \underset{\sim}{\boldsymbol{\varepsilon}} \tag{76}$$

$$= \Delta \varepsilon^e + \sum_{s=1}^{N_{slip}} \underset{\sim}{\boldsymbol{m}}^s \Delta \upsilon^s sign(\tau^s - x^s) + \sum_{s=1}^{N_{planes}} \Delta \delta^s_c \underline{\boldsymbol{n}}^s_d \otimes \underline{\boldsymbol{n}}^s_d + \Delta \delta^s_i \underline{\boldsymbol{n}}^s_d \otimes \underline{\boldsymbol{l}}^s_{d_i} \tag{77}$$

$$R_{\upsilon^s} = \Delta \upsilon^s - \Delta t \left\langle \frac{\Phi^s}{K} \right\rangle^n \tag{78}$$

$$R_{\delta_c^s} = \Delta\delta_c^s - \Delta t \left\langle \frac{f_c^s}{K_d} \right\rangle^{n_d} sign(\underline{\boldsymbol{n}}_d^s \cdot \underset{\sim}{\boldsymbol{\sigma}} \cdot \underline{\boldsymbol{n}}_d^s) \tag{79}$$

$$R_{\delta_i^s} = \Delta\delta_c^i - \Delta t \left\langle \frac{f_i^s}{K_d} \right\rangle^{n_d} sign(\underline{\boldsymbol{n}}_d^s \cdot \underset{\sim}{\boldsymbol{\sigma}} \cdot \underline{\boldsymbol{l}}_{d_i}^s) \tag{80}$$

$$R_{\delta_{cum}^s} = \Delta\delta_{cum} - \Delta \left(\sum_{s=1}^{N_{planes}} \left|\delta_c^s\right| + \left|\delta_1^s\right| + \left|\delta_2^s\right| \right) \tag{81}$$

$$[J] = \frac{\partial\{R\}}{\partial\{\Delta\nu\}} = 1 - \Delta t \left. \frac{\partial\{\dot{\nu}\}}{\partial\{\Delta\nu\}} \right|_{t+\Delta t} \tag{82}$$

where $\{R\}^T = \left[R_{\varepsilon^e},\ R_{\upsilon^s},\ R_{\delta_c^s},\ R_{\delta_i^s},\ R_{\delta_{cum}} \right]$ and ν stands for the internal state variables to be integrated locally. Then, the Jacobian matrix becomes

$$[J] = \begin{pmatrix} \frac{\partial R_{\varepsilon^e}}{\partial\Delta\varepsilon^e} & \frac{\partial R_{\varepsilon^e}}{\partial\Delta\upsilon^s} & \frac{\partial R_{\varepsilon^e}}{\partial\Delta\delta_c^s} & \frac{\partial R_{\varepsilon^e}}{\partial\Delta\delta_i^s} & \frac{\partial R_{\varepsilon^e}}{\partial\Delta\delta_{cum}} \\ \frac{\partial R_{\upsilon^s}}{\partial\Delta\varepsilon^e} & \frac{\partial R_{\upsilon^s}}{\partial\Delta\upsilon^e} & \frac{\partial R_{\upsilon^s}}{\partial\Delta\delta_c^s} & \frac{\partial R_{\upsilon^s}}{\partial\Delta\delta_i^s} & \frac{\partial R_{\upsilon^s}}{\partial\Delta\delta_{cum}} \\ \frac{\partial\delta_c^s}{\partial\Delta\varepsilon^e} & \frac{\partial\delta_c^s}{\partial\Delta\upsilon^e} & \frac{\partial\delta_c^s}{\partial\delta_c^s} & \frac{\partial\delta_c^s}{\partial\delta_{cum}} & \frac{\partial\delta_c^s}{\partial\delta_{cum}} \\ \frac{\partial\delta_i^s}{\partial\Delta\varepsilon^e} & \frac{\partial\delta_i^s}{\partial\Delta\upsilon^e} & \frac{\partial\delta_i^s}{\partial\delta_c^s} & \frac{\partial\delta_i^s}{\partial\delta_i^s} & \frac{\partial\delta_i^s}{\partial\delta_{cum}} \\ \frac{\partial\delta_{cum}}{\partial\Delta\varepsilon^e} & \frac{\partial\delta_{cum}}{\partial\Delta\upsilon^e} & \frac{\partial\delta_{cum}}{\partial\Delta\delta_i^s} & \frac{\partial\delta_{cum}}{\partial\Delta\delta_c^s} & \frac{\partial\delta_{cum}}{\partial\Delta\delta_{cum}} \end{pmatrix} \tag{83}$$

After convergence, the θ-method allows the calculation of the tangent matrix of the behaviour. R can be decomposed into two parts as

$$\{R\} = \{R_i\} - \{R_e\} \tag{84}$$

where R_e corresponds to the applied load. After the convergence (i.e. $\{R\} \approx \{0\}$) an infinitesimal variation can be applied to the residual equation such as

$$\delta\{R\} = \{0\} = \delta\{R_i\} - \delta\{R_e\} \tag{85}$$

which can be rewritten in the form:

$$\delta\Delta v_{int} = [J]^{-1}\, \delta\{R_e\} \tag{86}$$

For the calculation of elastic strain increment, the above relation reads

$$\delta\Delta\underset{\sim}{\boldsymbol{\varepsilon}}^e = \underset{\sim}{\underset{\sim}{\boldsymbol{J}}}_e \delta\Delta\underset{\sim}{\boldsymbol{\varepsilon}}, \quad \delta\Delta\underset{\sim}{\boldsymbol{\sigma}} = \underset{\sim}{\underset{\sim}{\boldsymbol{C}}} : \underset{\sim}{\underset{\sim}{\boldsymbol{J}}}_e \delta\Delta\underset{\sim}{\boldsymbol{\varepsilon}} \tag{87}$$

Note that a consistent tangent matrix can directly be obtained from $[\underset{\sim}{\underset{\sim}{\boldsymbol{C}}} : \underset{\sim}{\underset{\sim}{\boldsymbol{J}}}_e]$. A more comprehensir presentation of this systematic numerical integration method can be found in [3].

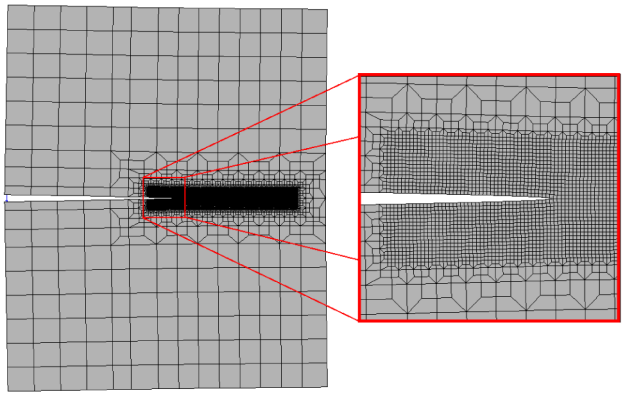

Fig. 3. FE mesh of a CT-like specimen created by ZeBuLoN GUI.

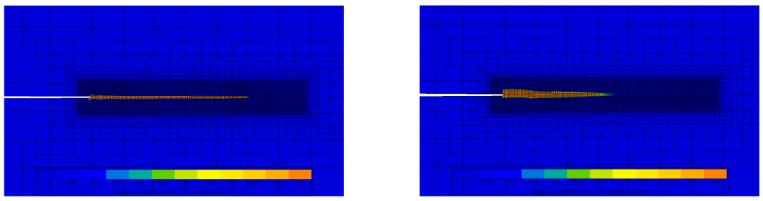

Fig. 4. Crack growth in a 2D single crystal CT-like specimen with a single cleavage plane aligned through the horizontal axis under vertical tension. Field variable δ. (Left) $A = 100$ MPa·mm^2, $H = -20000$ MPa, $^{\chi}H = 30000$ MPa; (Right) $A = 150$ MPa·mm^2, $H = -10000$ MPa, $^{\chi}H = 30000$ MPa.

5 Numerical Examples

As a 2D example, a single crystal CT-like specimen under tension is analysed. The corresponding FE mesh is given in Figure 3. Analyses are performed for two different crack widths, obtained by furnishing different material parameters which control the characteristic length. The propagation of a crack, corresponding stress fields and the comparison with classical elastic solutions are given in Figure 5. This comparison shows that the microdamage model is able to reproduce the stress concentration at the crack tip except very close to the crack tip where finite stress values are predicted.

Another 2D example, namely a plate under uniaxial tension with several cleavage planes, is investigated (see Figure 6). In order to trigger localization, an initial geometric defect is created on the left edge. First, a cleavage plane is oriented at 30° from the horizontal axis. FEA results show that localization path is perfectly matching with the cleavage plane and the size of the localization band is controlled by ω in (65) (Figure 6, left). Second, two orthogonal cleavage planes are placed with an orientation of 45° from the horizontal axis representing $\{111\}$ planes. For the former case, damage is coupled with plasticity and two localization bands merge together and form a straight crack path which can be considered as a type of ductile crack

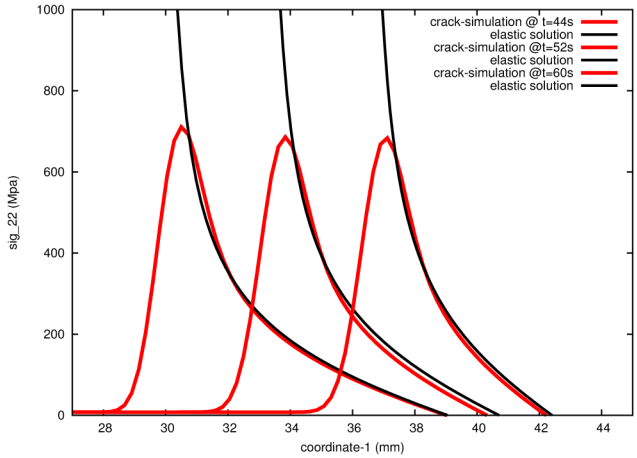

Fig. 5. Evolution of the crack and the stress fields in a CT-like specimen compared with corresponding elastic solutions.

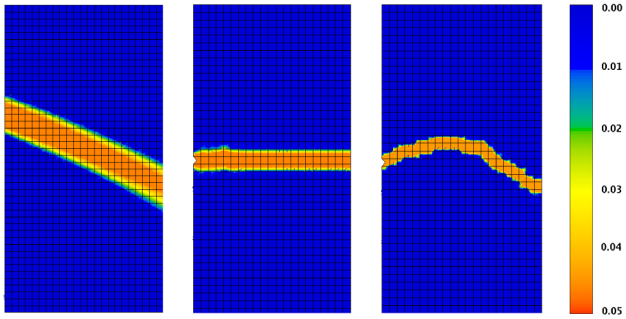

Fig. 6. Crack growth in a 2D single crystal block with a single inclined cleavage plane (left) and two orthogonal planes oriented at 45 degrees (middle and right) under vertical tension with 10% strain. Field variable δ.

(Figure 6, middle). For the latter case, plasticity is excluded from the calculation and crack path is allowed to choose its path between the orthogonal planes which results in a brittle type of crack propagation (Figure 6, right).

In [2], FEA of a CT-like fracture mechanics specimen under tension was considered. The analysis was done by creating a cleavage plane parallel to the horizontal axis and the loading was performed from the center of the pin. For a given characteristic length (associated with parameters $A = 200\,\text{MPa}\cdot\text{mm}^2$, $H = -16000\,\text{MPa}$, ${}^{\chi}H = 50000\,\text{MPa}$), mesh refinement of the specimen lead to a unique fracture curve and a finite size crack width, as shown in Figure 7 and in the loading curves in [2].

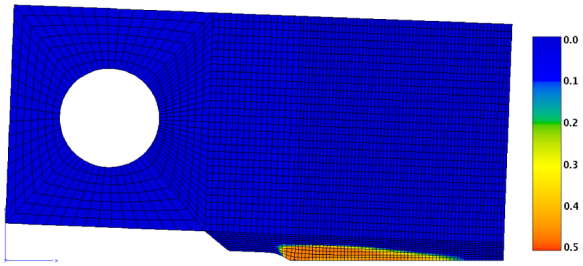

Fig. 7. Crack growth in a CT-like specimen under tension under vertical tension with 8% strain. Field variable δ.

6 Conclusion

The proposed systematic treatment of the thermomechanics of continua with additional degrees of freedom leads to model formulations ranging from micromorphic to phase field models. In particular, a general framework for the introduction of dissipative processes associated with the additional degrees of freedom has been proposed. If internal constraints are enforced on the relation between macro and microvariables in the micromorphic approach, standard second gradient and strain gradient plasticity models can be retrieved as shown in [11].

As a variant of micromorphic continuum, microdamage continuum and its regularization capabilities for the modelling of crack propagation in single crystals have been studied. First, a crystallographic constitutive model which accounts for continuum damage with respect to fracture planes has been presented. Then, the theory has been extended from classical continuum to microdamage continuum, respectively. It has been shown that the approach can be a good candidate for solving mesh dependency and the prediction of final fracture. Analytical fits and numerical results showed that the theory is well suited for FEA and possesses a great potential for the future modelling aspects. Comparison with available data on crack growth especially cyclic loading in nickel-based superalloys, will be decisive to conclude on the ability of the approach to reach realistic prediction of component failure.

References

1. K. Ammar, B. Appolaire, G. Cailletaud, F. Feyel, and F. Forest. Finite element formulation of a phase field model based on the concept of generalized stresses. *Computational Materials Science*, 45:800–805, 2009.
2. O. Aslan and S. Forest. Crack growth modelling in single crystals based on higher order continua. *Computational Materials Science*, 45:756–761, 2009.
3. J. Besson, G. Cailletaud, J.-L. Chaboche, S. Forest, and M. Blétry. *Non-Linear Mechanics of Materials*. Springer, 2009.
4. J. Besson, R. Leriche, R. Foerch, and G. Cailletaud. Object-oriented programming applied to the finite element method. Part II: Application to material behaviours. *Rev. Eur. Elem. Finis*, 7:567–588, 1998.

5. G. Cailletaud, S. Forest, D. Jeulin, F. Feyel, I. Galliet, V. Mounoury, and S. Quilici. Some elements of microstructural mechanics. *Computational Materials Science*, 27:351–374, 2003.
6. B.D. Coleman and W. Noll. The thermodynamics of elastic materials with heat conduction and viscosity. *Arch. Rational Mech. and Anal.*, 13:167–178, 1963.
7. T. Dillard, S. Forest, and P. Ienny. Micromorphic continuum modelling of the deformation and fracture behaviour of nickel foams. *European Journal of Mechanics A/Solids*, 25:526–549, 2006.
8. R.A.B. Engelen, M.G.D. Geers, and F.P.T. Baaijens. Nonlocal implicit gradient-enhanced elasto-plasticity for the modelling of softening behaviour. *International Journal of Plasticity*, 19:403–433, 2003.
9. A.C. Eringen. *Microcontinuum Field Theories*. Springer, New York, 1999.
10. A.C. Eringen and E.S. Suhubi. Nonlinear theory of simple microelastic solids. *Int. J. Engng Sci.*, 2:189–203, 389–404, 1964.
11. S. Forest. The micromorphic approach for gradient elasticity, viscoplasticity and damage. *ASCE Journal of Engineering Mechanics*, 135:117–131, 2009.
12. S. Forest and R. Sievert. Elastoviscoplastic constitutive frameworks for generalized continua. *Acta Mechanica*, 160:71–111, 2003.
13. M.G.D. Geers, R. de Borst, W.A.M. Brekelmans, and R.H.J. Peerlings. On the use of local strain fields for the determination of the intrinsic length scale. *Journal de Physique IV*, 8:Pr8–167–174, 1998.
14. N. Germain, J. Besson, and F. Feyel. Simulation of laminate composites degradation using mesoscopic non-local damage model and non-local layered shell element. *Modelling and Simulation in Materials Science and Engineering*, 15:S425–S434, 2007.
15. P. Germain. La méthode des puissances virtuelles en mécanique des milieux continus, première partie: Théorie du second gradient. *J. de Mécanique*, 12:235–274, 1973.
16. P. Germain, Q.S. Nguyen, and P. Suquet. Continuum thermodynamics. *Journal of Applied Mechanics*, 50:1010–1020, 1983.
17. M.E. Gurtin. Generalized Ginzburg–Landau and Cahn–Hilliard equations based on a microforce balance. *Physica D*, 92:178–192, 1996.
18. C.B. Hirschberger and P. Steinmann. Classification of concepts in thermodynamically consistent generalized plasticity. *ASCE Journal of Engineering Mechanics*, 135:156–170, 2009.
19. N. Marchal, S. Flouriot, S. Forest, and L. Remy. Crack-tip stress-strain fields in single crystal nickel-base superalloys at high temperature under cyclic loading. *Computational Materials Science*, 37:42–50, 2006.
20. N. Marchal, S. Forest, L. Rémy, and S. Duvinage. Simulation of fatigue crack growth in single crystal superalloys using local approach to fracture. In D. Steglich, J. Besson, and D. Moinereau (Eds.), *Local Approach to Fracture*, 9th European Mechanics of Materials Conference, Euromech-Mecamat, Moret-sur-Loing, France. Presses de l'Ecole des Mines de Paris, pp. 353–358, 2006.
21. G.A. Maugin. The method of virtual power in continuum mechanics: Application to coupled fields. *Acta Mechanica*, 35:1–70, 1980.
22. G.A. Maugin. *Thermomechanics of Nonlinear Irreversible Behaviors*. World Scientific, 1999.
23. R.D. Mindlin. Micro-structure in linear elasticity. *Arch. Rat. Mech. Anal.*, 16:51–78, 1964.
24. H.B. Mühlhaus. *Continuum Models for Materials with Microstructure*. Wiley, 1995.

25. R.H.J. Peerlings, M.G.D. Geers, R. de Borst, and W.A.M. Brekelmans. A critical comparison of nonlocal and gradient-enhanced softening continua. *Int. J. Solids Structures*, 38:7723–7746, 2001.
26. R.H.J. Peerlings, T.J. Massart, and M.G.D. Geers. A thermodynamically motivated implicit gradient damage framework and its application to brick masonry cracking. *Comput. Methods Appl. Mech. Engrg.*, 193:3403–3417, 2004.